Flexible Unfolding of Circular Structures for Rendering Textbook-Style Cerebrovascular Maps

Leonhard Rist[1,2(✉)], Oliver Taubmann[2], Hendrik Ditt[2], Michael Sühling[2], and Andreas Maier[1]

[1] Friedrich-Alexander-Universität Erlangen-Nürnberg, Erlangen, Germany
leonhard.rist@fau.de
[2] CT R&D Image Analytics, Siemens Healthineers, Forchheim, Germany

Abstract. Comprehensive, contiguous visualizations of the main cerebral arteries and the surrounding parenchyma offer considerable potential for improving diagnostic workflows in cerebrovascular disease, e.g., for fast assessment of vascular topology and lumen in stroke patients. Unfolding the brain vasculature into a 2D overview is, however, infeasible using common Curved Planar Reformation (CPR) due to the circular structure of the Circle of Willis (CoW) and the spatial configuration of the vessels typically rendering them unsuitable for mapping onto simple geometric primitives. We propose CeVasMap, extending the As-Rigid-As-Possible (ARAP) deformation by a smart initialization of the required mesh to map the CoW as well as a merging of neighboring vessels depending on the resulting degree of distortion. Otherwise, vessels are unfolded and attached individually, creating a textbook-style overview image. We provide an extensive distortion analysis, comparing the vector fields of individual and merged unfoldings of each vessel to their CPR results. In addition to enabling unfolding of circular structures, our method is on par in terms of incurred distortions to optimally oriented CPRs for individual vessels and comparable to unfavorable CPR orientations when merging the complete CoW with a median distortion of 65 µm/mm.

Keywords: Vessel unfolding · Distortion · Cerebrovascular disease

1 Introduction

Assessing vascular lumen and topology is among the most critical tasks for timely diagnosis of acute cerebrovascular disease, including the detection of vessel occlusions (e.g., by left-right hemisphere comparisons) and the assessment of redundant blood flow paths via the communicating arteries [2] in stroke diagnosis. Identifying impairments such as thrombi for stroke analysis in the nested cerebral artery system from a Computed Tomography Angiography (CTA) scan

Supplementary Information The online version contains supplementary material available at https://doi.org/10.1007/978-3-031-43904-9_71.

H. Greenspan et al. (Eds.): MICCAI 2023, LNCS 14224, pp. 737–746, 2023.
https://doi.org/10.1007/978-3-031-43904-9_71

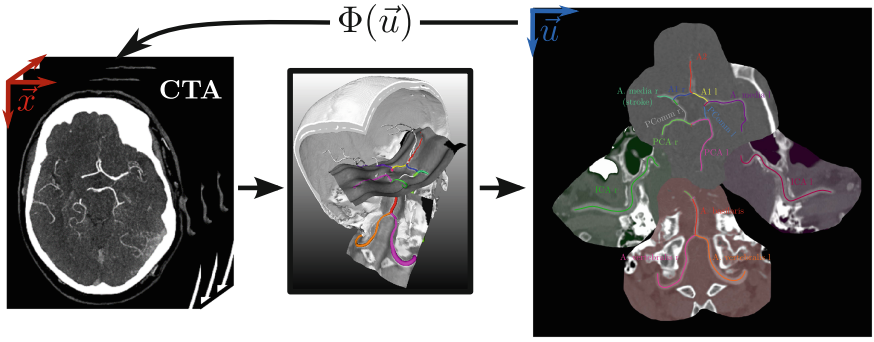

Fig. 1. Unfolding of a labeled cerebrovascular vessel graph from a CTA volume to a 2D overview map with centerline, label and area overlay.

can be inefficient due to the need to interact with the visualization to properly review all relevant vessels. Instead of manually tracking individual vessels across multiple slices, it is also possible to project their complete lumen into a single image plane, called unfolding. Yet, analyzing the global appearance of all cerebral vessels at once, primarily the main arteries forming and surrounding a ring structure called Circle of Willis (CoW; exists in many common norm variants) can be equally important.

However, this circular structure cannot be properly unfolded with the common Curved Planar Reformation (CPR) technique [3], its untangled extension or through conformal mappings [15] due to imperfect circle symmetry leading to different lengths when unfolding the opposing sides. Hence, unfolding is done individually per vessel [12] or by simply showing the configuration in bullet-maps [9]. For many other anatomical structures exist already flattening techniques [4], e.g., using ray-casting for rip unfolding [8]. Relevant unfolding techniques in the brain include aneurysm maps [10] or cortex flattening using mesh deformation [1].

In computer graphics, disk-like mesh parameterization [6] or angle-preserving conformal maps [7] can be used to bring objects in a planar representation. For the involved task of mesh deformation, algorithms such as the As-Rigid-As-Possible (ARAP) method [13] aim to preserve shape during the process, which was already adapted for medical purposes such as pelvis [5] or heart (vessel) unfolding. However, as shown in the vessel tree in Fig. 1, cerebral vessels often bifurcate in perpendicular directions or run in parallel, eliminating the possibility to use simple geometric primitives for the whole CoW. Consequently, comprehensive, contiguous unfoldings of the cerebrovascular system have not been demonstrated before.

This work aims to generate a complete textbook-style vessel map of the cerebral vasculature along the CoW to generate a standardized overview image. Building on the ARAP algorithm, we propose CeVasMap (C*erebral* Vas*culature* Map*ping*): a method to unfold circular structures which can be flexibly extended with peripheral vessels, either by including them in the unfolding directly or attaching them individually. This results in locally restricted distortions, retain-

ing curvature information and keeping most of the image distortion-free. Given labeled centerlines, we create a smooth initial mesh with optimal viewing direction dependent on the vessels' principal components and deform it as rigidly as possible to jointly display all vessels of interest. We provide a comprehensive vessel-level evaluation by calculating and visualizing the distortions resulting from the underlying 2D-3D vector field.

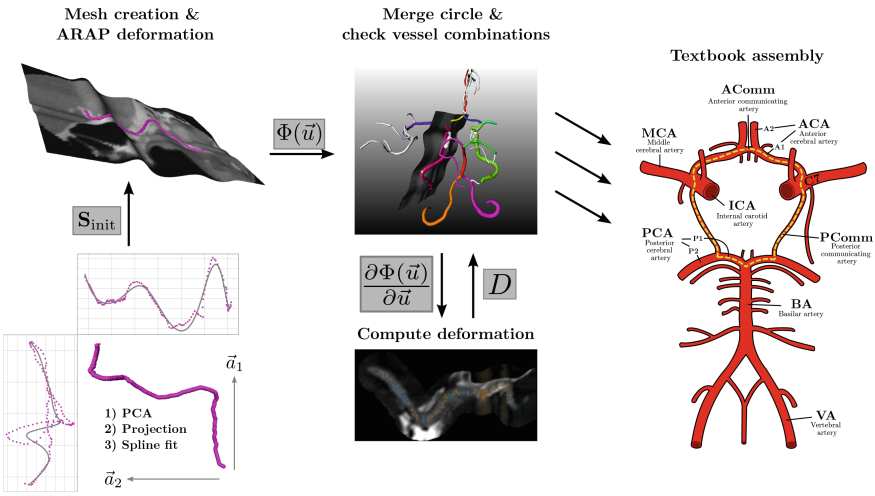

Fig. 2. Unfolding pipeline for an individual vessel (ICA), starting from centerline (left). CoW textbook scheme (right), circle highlighted in yellow. (Color figure online)

2 Methods

2.1 Data

We use a data set consisting of 30 CTA scans (Siemens Somatom Definition AS+) from stroke patients (63.3% males, $74,5 \pm 12,5$ years, 33.3% MCA stroke) with an average voxel spacing of 0.634 mm (in-plane) and 0.57 mm (axial). The brain vasculature is segmented and labeled [11,14]. An example is displayed in the CoW scheme in Fig. 2.

2.2 Rationale

The goal of this work is to generate a single 2D image which contains all vessels of interest jointly with the surrounding parenchyma. Hence, the task at hand is to find an unfolding transformation $\Phi(\vec{u}) = \vec{x} : \mathbb{R}^2 \rightarrow \mathbb{R}^3$ mapping from a 2D position $\vec{u}$ in the unfolded target image to its 3D CTA volume location $\vec{x}$. The corresponding coordinate systems are illustrated in Fig. 1.

Clinically useful images should be merged at the bifurcations to allow consistent path tracing. Additionally, anatomical properties such as vessel curvature

should be preserved whereas strong distortions are to be avoided. The main concept of the proposed method is the generation of a joint mapping for the CoW. Further attached vessels can then be merged to it to form a complete overview at the cost of a higher distortion, see Sect. 2.3. For configurations that lead to strong distortions, outer vessels are unfolded individually and attached to the main component. Their arrangement is inspired by the common textbook CoW schematic for better orientation, see Fig. 2. Unfolding of individual as well as combined vessels is described in Sect. 2.4, merging and image assembly in Sect. 2.5.

2.3 Measuring Distortions

An image resulting from a transformation Φ lacks a consistent pixel spacing, the specified one is simply an average from the covered 3D distances, hence pixel distances deviating from that average are distorted. We compute distortion metrics on the vector field Φ to guide the decision process during the merging and for the evaluation. Since conventional metrics to find sources and sinks such as the Jacobian determinant can only be calculated for equidimensional Φs, we compute a scalar metric d per pixel $\vec{u} = (u, v)$ by deriving the transformation w.r.t. both image directions $\frac{\partial \Phi(\vec{u})}{\partial \vec{u}} \in \mathbb{R}^{3\times 2}$ and applying the Frobenius norm,

$$d_{uv} = ||\frac{\partial \Phi(\vec{u})}{\partial \vec{u}}||_F - \alpha = \begin{cases} > 0 & \text{locally stretched,} \\ = 0 & \text{no distortion,} \\ < 0 & \text{locally contracted.} \end{cases} \tag{1}$$

When sampling a 2D image of size $N \times M$ with isotropic sampling μ, a pixel gradient of 1 in one image direction implies a sampling in 3D with μ, meaning no distortion. To normalize distortion-free values of d_{uv} to 0, the constant $\alpha = \sqrt{2}$ is subtracted. A global image metric is then calculated as $D = \frac{1}{N \cdot M} \sum_{u,v}^{N,M} |d_{uv}|$.

2.4 ARAP Vessel Unfolding

CPR unfolding can lead to displeasing results, e.g., at highly curved segments perpendicular to image read-out direction, impairing the quality of the displayed lumen and parenchyma in the whole image row, see bottom right in Fig. 4. Instead of sampling read-out points $\vec{p} \in \mathbb{R}^3$ line by line starting from the centerline as done by Kanitsar et al. [3], one could also assume a continuous (triangular) mesh surface $\mathbf{S}$ with $\vec{p}_i$ being the vertex position i and downstream image read-out points. One would then find and deform an initial mesh representation, fitting it to the vessels of interest. When deforming such a mesh into $\mathbf{S}'$ with $\vec{p}\,'_i$, one has direct control of the rigidity between neighboring vertices by measuring the local rigidity energy [13]:

$$E(\mathbf{S}') = \sum\nolimits_{i=1..N} w_i \sum\nolimits_{j \in \mathcal{N}(i)} w_{ij} ||(\vec{p}_i\,' - \vec{p}_j\,') - \mathbf{R}_i(\vec{p}_i - \vec{p}_j)||^2 \tag{2}$$

with $\mathcal{N}(i)$ being the 1-step neighborhood of i. By minimizing the norm of the rigid error on the right-hand side, one can approximate a rigid transformation,

since actual rigidness is infeasible. For the derivation of the rotation $\mathbf{R}_i$ and the weights w_{ij} and w_i, we refer to Sorkine et al. [13].

On one hand, we lack a fully defined object surface due to our sparse vessel structure. On the other hand, staying close to a meshed plane would mimic multiplanar reformation images and help with the orientation. Since this structure would lead to strong distortion due to its simplicity compared to the centerlines, we define our read-out mesh in a two-step approach. First, we use the principal component vectors stored column-wise in $\mathbf{A} \in \mathbb{R}^{3\times3}$, using column $\vec{a}_3$ as the optimal viewing direction by projecting the points $\vec{c}_j$ from the set of centerline points $j \in \mathcal{C}$ along the two maximum principal components to acquire two 1D distributions $k_{1,2}$, see Fig. 2. To create a smooth surface independent of point density in certain areas, a B-spline b_k is fitted for each of the distributions with the number of knots dependent on the vessel length. Sampling from those functions creates an initial smooth shape $\mathbf{S}_{\text{init}}$ with

$$\vec{p}_{u,v}^{\,(\text{init})} = \mathbf{A}\vec{q}_{u,v} + \vec{\bar{c}} \quad \text{with} \quad \vec{q}_{u,v} = (\mu u, \mu v, b_1(u) + b_2(v))^\top \tag{3}$$

as vertex positions where u and v are sampled uniformly from $[-\frac{N}{2}, \frac{N}{2}]$, $[-\frac{M}{2}, \frac{M}{2}]$ and $\vec{\bar{c}}$ is the centerline mean position. To avoid escalating border regions, the last value of $\vec{q}_{u,v}^{\,(\text{init})}$ is set to 0 outside of the centerline bounding box. Next, $\mathbf{S}_{\text{init}}$ is deformed to contain all vessel points following the ARAP minimization in Eq. 2 by restraining a subset of $\vec{p}_i\,'$ to $\vec{c}_j$. Volume intensities can be read out at the vertex positions of the resulting mesh $\mathbf{S}$, forming the target vector field $\Phi_{\text{CeVasMap}}(\vec{u}) = \vec{p}$ beginning from the unfolded image.

2.5 Merging and Image Assembly

In principle, the described approach can be applied to all vessels of interest at once, introducing high distortion at nearly perpendicular bifurcations. Due to a varying amount of contrast agent; scan, segmentation or labeling quality; or occlusions in stroke, the vessels can differ greatly in length. Long, curved structures influence the unfolding more severely since $\mathbf{S}_{\text{init}}$ has to adapt to more points $\vec{c}_j$, increasing the initial fitting error. In such cases, individual vessels are unfolded separately to maintain sufficient image quality and included in the cerebral vessel map at the position and rotation angle according to the textbook schematic, see Fig. 2. To obtain a standardized image, the CoW (AComm, A1, PComm, P1, ICA C7) is always unfolded jointly to form the center of the image. Afterwards, vessels can be merged based on their importance to the task at hand and by setting an upper threshold $D < \beta$. An exemplary strategy in stroke scenarios would encourage a merging of the often-affected MCAs, together with the anterior part, followed by the PCAs.

2.6 Evaluation

The distortion by the proposed transformation and the baseline is evaluated quantitatively and qualitatively using the metrics from 2.3. The baseline method

is the CPR transformation $\Phi_{\text{CPR}}(\vec{u})$ following Kanitsar et al. [3], linearly sampling image rows starting from equidistant points on the centerline. We present the results of both the best and worst CPR viewing. All vessels are unfolded individually with approx. the same isotropic spacing (0.256 mm) and zoom level. Metrics are computed only for pixels that are sampled from a conservatively chosen radius of 10 mm around the centerline in the volume, since larger images favor our approach due to its distortion-free property in areas distant to the vessel.

The pixel-wise metric d_{uv} is used to visually inspect the results. Quantitatively, distortion is assessed showing the mean-like metric D as a distribution over all 30 patients. Additionally, the median of $|d_{uv}|$ per vessel unfolding averaged over all patients is shown to also investigate the maximal distortion of the lesser affected half of the pixels. To assess the expected distortion increase caused by merging, we split the cerebral vessels into two groups: For the CoW vessel segments (merged by default), D and median metric are calculated over the image patches of each vessel, both for individual unfoldings and extracted from the merging. Similarly, the D-distribution and frequency of successfully merging outer vessel pairs to the unfolded circle structure is reported when setting an upper distortion threshold of $D < 25\%$ for the vessel of interest. To avoid that simultaneously merged vessel pairs influence each other or the circle, we compute $\mathbf{S}_{\text{init}}$ only from the circle and then merge vessel pairs using ARAP. This also eliminates the need to evaluate distortions for all possible vessel combinations.

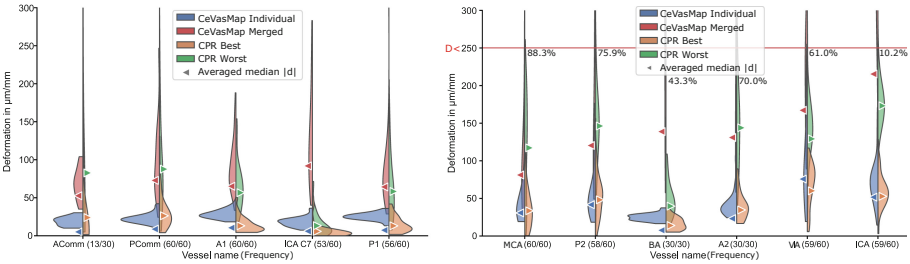

(a) Circle-forming vessels (b) Outer vessels

Fig. 3. Quantitative distortion metrics per individual vessel unfolding over all 30 patients. D is shown as violin distributions comparing our method with best and worst CPR angle. Averaged medians are computed from $|d_{uv}|$. (a) Only the circle is merged. (b) Vessel pairs are merged to circle. Fraction of merged vessels and median distortions provided for merged vessels with $D < 25\%$ (red threshold).

3 Results

Quantitative metrics per vessel (pair) are presented in Fig. 3 and a qualitative example of a cerebral vessel map with distortion heatmaps is shown in Fig. 4. Even using the narrow 10 mm distance threshold, CeVasMap consistently has

lower median values than the best CPR angles, except for the short ICA C7 and the VA. Within the CoW, all median values are below 10 µm/mm distortion, the outer vessels are all below 50 µm/mm, except for VA. However, the distributions generally show a slightly lower mean for CPR (best), together with a lower average standard deviation for all vessels. Especially for long vessels (MCA, VA, P2, ICA), we observe higher maximum values in the D-distribution and standard deviation. Qualitative analysis (cf. the example in Fig. 4) confirms the theoretical properties of the two compared approaches. While our approach has locally restricted distortions around the centerline (ARAP target points) with a higher amplitude, CPR affects the distortion along an image row, potentially resulting in inflated vessels due to oversampling inside the lumen at curvature points, see Fig. 4 on the bottom right. For CeVasMap, high distortion in the VA occurs a the end of the labeled vessel, caused by absent neighboring target points. Slight distortions for our approach outside of the vessel (orange shade in ICA r) are caused by the sampling of $\mathbf{S}_{\text{init}}$. For more qualitative examples, see Suppl. Fig. 1.

When merging the CoW (Fig. 3a), the median distortions (65 µm/mm for the complete circle) naturally increase but are still almost on par with (P1, A1) or even outperform (AComm, PComm) the individually unfolded worst CPR angle, except for the ICA C7 segment which is often oriented nearly perpendicular to the remaining circle segments. Using our threshold for the outer vessels, it is possible to merge the MCA in 88.3% of the cases. Vessels perpendicular to the CoW plane could however only be merged in 10.2% (ICA) or 43.3% (BA).

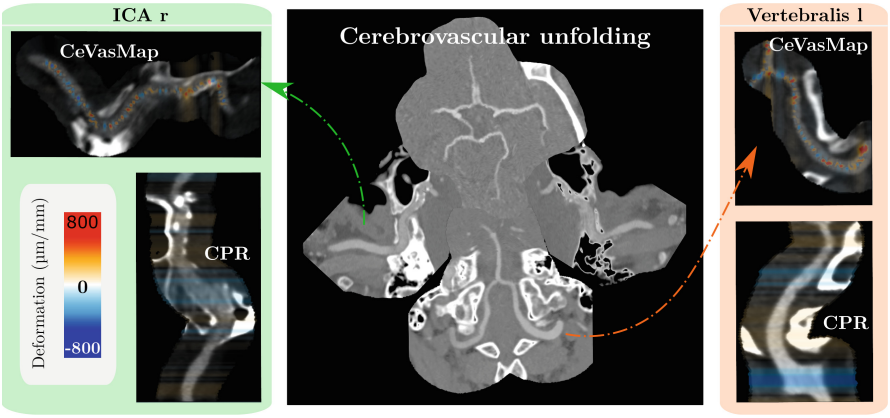

Fig. 4. Exemplary qualitative result of cerebrovascular unfolding: Merged circle with A2, MCA and PCA. ICAs unfolded individually. BA and VA are merged together independent of CoW. Comparison to CPR with distortion heatmap (left/right) using a global color scale (bottom left).

4 Discussion and Conclusion

We present CeVasMap, a flexible method to generate textbook-style vessel maps of the main cerebral arteries, including an unfolding technique capable of displaying circular structures infeasible for the widely used CPR approach. To unfold individual vessels or vessel groups, a read-out mesh is generated by fitting splines to centerline projections along the principal components. This initial mesh is deformed using the ARAP algorithm to display the full vessel lumen. In our approach, we suggest jointly mapping the inner circular structure of the CoW by default and extending it with outer vessels depending on the task at hand and the introduced distortion. For this purpose, a gradient-based distortion metric is calculated on the 2D-3D unfolding vector field, which also facilitates quantitative and qualitative assessment of the mapping quality.

The method results in higher standard deviations and slightly higher mean values of the proposed gradient-based distortion metric D compared to the best possible CPR angle. However, CeVasMap generally achieves lower median values ($\leq 10\,\mu m/mm$ for the CoW vessels, and mostly $\leq 50\,\mu m/mm$ for the longer outer segments), meaning larger parts of the image are distortion-free. Even when merging the complete CoW (average distortion median of $65\,\mu m/mm$), our method can still compete with the individual CPR unfolding using less favorable angles. When merged with the CoW, distortion for outer vessels, especially those nearly perpendicular to the CoW plane, is quite high, and only the MCAs, PCAs and A2 arteries achieve satisfying results due to their orientation. For instance, the ICA could only be merged in 10.2% while the MCA has a 88.3% success rate with our proposed threshold. To assess only distortions close to the structures of interest, i.e., the vessels, we evaluated our metrics within a narrow corridor around them. When generating full cerebrovascular unfoldings, one would rather unfold more parenchyma for a hole-free image (cf. Fig. 4), leading to a significant improvement of our metrics.

Rotating the unfolded views as often done in CPR is in theory feasible with our approach—by rotating the principal components $\mathbf{A}$—but is not expected to give pleasing results as ARAP target points are rotated out-of-plane. Insufficient unfolding length or asymmetric manifestations of vessel pairs can occur due to segmentation or labeling inconsistencies. Nevertheless, our method is more robust against segmentation or labeling errors causing strongly curved, incorrect or fistula-like pathways. In contrast to CPR, our method is robust against varying centerline point distances and inconsistent centerline point ordering.

The flexible nature of our approach can also be used to focus on the arteries of interest by merging them selectively and keeping the remaining vessels separate but arranged intuitively inspired by textbook presentations, effectively reducing overall distortion. Such a selective merging could also be done interactively as, compared to higher computation times for segmentation and labeling, most unfolding steps are parallelizable and can be computed in few seconds.

The clinical applications of a cerebrovascular overview map are manifold. The configuration of the CoW and surrounding major vessels is visualized, giving insight into the collateral blood supply or supporting contralateral comparisons

for time-critical stroke detection while being able to view the vessel lumen and its pathologies at a glance. To evaluate challenging real-world scenarios, this work is specifically tested using stroke data as it one of the main reasons for topological impairments of the CoW. This unique representation (compared to volume renderings or slice images) of the cerebrovascular system can be useful for diagnostic reports, comparing patients, disease tracking or to simply to mark locations of possible findings. The maps are also helpful for navigation within the volume as the transformation allows us to readily display multiplanar reformations of the original volume centered at 3D positions corresponding to (manually selected) positions in the unfolded overview image ("picking"). Finally, this condensed lower-dimensional representation could also be beneficial for training downstream deep learning models more efficiently.

Acknowledgments. We would like to acknowledge our collaborators at the University Hospital Schleswig-Holstein in Lübeck for providing the data used in this work. It was collected in a retrospective study which received Institutional Review Board approval prior to starting. The need for informed consent was waived.

References

1. Balasubramanian, M., Polimeni, J.R., Schwartz, E.L.: Near-isometric flattening of brain surfaces. NeuroImage **51**(2), 694–703 (2010). https://doi.org/10.1016/j.neuroimage.2010.02.008
2. Gunnal, S.A., Farooqui, M.S., Wabale, R.N.: Anatomical variability of the posterior communicating artery. Asian J. Neurosurg. **13**, 363 (2018). https://doi.org/10.4103/AJNS.AJNS_152_16
3. Kanitsar, A., Fleischmann, D., Wegenkittl, R., Felkel, P., Groller, E.: CPR - curved planar reformation. In: IEEE Visualization, 2002 (VIS 2002), pp. 37–44 (2002). https://doi.org/10.1109/VISUAL.2002.1183754
4. Kreiser, J., Meuschke, M., Mistelbauer, G., Preim, B., Ropinski, T.: A survey of flattening-based medical visualization techniques. Comput. Graph. Forum **37**, 597–624 (2018). https://doi.org/10.1111/cgf.13445
5. Kretschmer, J., Soza, G., Tietjen, C., Suehling, M., Preim, B., Stamminger, M.: ADR - anatomy-driven reformation. IEEE Trans. Visual. Comput. Graph. **20**(12), 2496–2505 (2014). https://doi.org/10.1109/TVCG.2014.2346405
6. Liu, L., Zhang, L., Xu, Y., Gotsman, C., Gortler, S.J.: A local/global approach to mesh parameterization. Comput. Graph. Forum **27**, 1495–1504 (2008). https://doi.org/10.1111/j.1467-8659.2008.01290.x
7. Lévy, B., Petitjean, S., Ray, N., Maillot, J.: Least squares conformal maps for automatic texture atlas generation. ACM Trans. Graph. **21**, 362–371 (2002). https://doi.org/10.1145/566654.566590
8. Martinke, H., et al.: Bone fracture and lesion assessment using shape-adaptive unfolding. In: Eurographics Workshop on Visual Computing for Biology and Medicine. The Eurographics Association (2017). https://doi.org/10.2312/vcbm.20171249
9. Miao, H., Mistelbauer, G., Nasel, C., Gröller, E.: Visual quantification of the circle of Willis: an automated identification and standardized representation. Comput. Graph. Forum **36**(6), 393–404 (2017). https://doi.org/10.1111/cgf.12988

10. Neugebauer, M., Gasteiger, R., Beuing, O., Diehl, V., Skalej, M., Preim, B.: Map displays for the analysis of scalar data on cerebral aneurysm surfaces. Comput. Graph. Forum **28**(3), 895–902 (2009). https://doi.org/10.1111/j.1467-8659.2009.01459.x
11. Rist, L., Taubmann, O., Thamm, F., Ditt, H., Sühling, M., Maier, A.: Bifurcation matching for consistent cerebral vessel labeling in CTA of stroke patients. Int. J. Comput. Assist. Radiol. Surg. **18**(3), 509–516 (2022). https://doi.org/10.1007/s11548-022-02750-9
12. Shen, M., et al.: Automatic cerebral artery system labeling using registration and key points tracking. In: Knowledge Science, Engineering and Management, pp. 355–367 (2020). https://doi.org/10.1007/978-3-030-55130-8_31
13. Sorkine, O., Alexa, M.: As-rigid-as-possible surface modeling. In: Proceedings of the Fifth Eurographics Symposium on Geometry Processing (SGP 2007), pp. 109–116. Eurographics Association, Goslar, DEU (2007). https://doi.org/10.2312/SGP/SGP07/109-116
14. Thamm, F., et al.: An algorithm for the labeling and interactive visualization of the cerebrovascular system of ischemic strokes. Biomed. Phys. Eng. Exp. **8**(6) (2022). https://doi.org/10.1088/2057-1976/ac9415
15. Zhu, L., Haker, S., Tannenbaum, A.: Flattening maps for the visualization of multibranched vessels. IEEE Trans. Med. Imaging **24**(2), 191–198 (2005). https://doi.org/10.1109/TMI.2004.839368